

Latent Heat Recovery from Oxygen-Combustion Flue Gas

Masahiro OSAKABE

Tokyo University of Mercantile Marine, Koutou-ku, Tokyo 135-8533, Japan
 Phone +81-3-5245-7404, FAX +81-3-5245-7336
 E-Mail osakabe@ipc.tosho-u.ac.jp

ABSTRACT

The most part of energy losses in a boiler is due to the heat released by the exhaust flue gas to atmosphere. The released heat consists of sensible and latent one. As a next generation boiler, the oxygen combustion boiler was planned and developed in Japan. The steam mass concentration of the oxygen-combustion flue gas was approximately 25% which value is higher than that of the air-combustion flue gas. The latent heat highly included in the flue gas is very important resource.

Based on the previous basic studies, a prediction method was proposed for the design of heat exchanger to recover the latent heat in the oxygen-combustion flue gas. The one-dimensional heat and mass balance calculation was conducted along the flow direction of flue gas in the heat exchanger. For the condensation of steam on heat transfer tubes, the modified Sherwood number taking account of the mass absorption effect on the wall was proposed. The heat and mass transfer on tubes was evaluated with the modified analogy correlation and the thermal resistance of the condensate film on tubes could be neglected. In the calculation, it was possible that the gas temperature merged with the dew point which was the saturation temperature corresponding to the partial pressure of steam in the flue gas. When the gas temperature decreased below the dew point, the condensation of steam in the flue gas took place and the released latent heat increased the gas temperature until the gas temperature coincided with the dew point.

The thermal-hydraulic behavior was experimentally studied in a heat exchanger for the latent heat recovery from a flue gas generated with the combustion of oxygen and A-oil. The parametric study varying the flue gas and feed water flow rate was conducted. The experimental results agreed well with the one-dimensional prediction proposed in this study.

NOMENCLATURE

C: mass concentration per fluid of a unit volume [kg/m³]
 C_p: specific heat [J/kg]
 d: outer diameter of tube [m]
 d_i: inner diameter of tube [m]
 D: mass diffusivity [m²/s]
 h_v: heat transfer coefficient [W/(m²K)]
 h_c: mass transfer coefficient [m/s]
 L_w: latent heat [J/kg]
 Nu: Nusselt number [= h_vd / λ]
 Nr: total number of stages
 P: pressure [Pa]
 q: heat flux [kW/m²]
 Pr: Prandtl number [= ν / κ]
 Re: Reynolds number [= ud / ν]
 S₁: spanwise pitch [m]
 S₂: flow-directional pitch [m]
 Sh: Sherwood number [= h_cd / D]
 Sc: Schmidt number [= ν / D]
 T: temperature [°C]
 u: velocity at minimum flow area [m/s]
 V: volumetric flow rate [m³/s]
 w: mass concentration per fluid of an unit mass [kg/kg]
 κ: thermal diffusivity [= λ / (ρC_p)]
 λ: heat conductivity [W/(mK)]
 μ: oxygen or air ratio
 ν: kinematic viscosity [m²/s]
 ρ: density [kg/m³]

subscript

a: atmosphere, C: condensation, COX: carbon dioxide and monoxide, d: dry gas, F: fuel, f: flue gas, i: condensation surface, V: convection, W: wall, N: standard condition at 0°C and atmospheric pressure, sat: saturated condition of steam, sub: subcooling, wt: wet gas

*Professor, Chair of Power System Engineering
 Copyright©2000 The American Institute of Aeronautics and Astronautics Inc. All rights reserved.

INTRODUCTION

The most part of energy losses in a boiler is due to the heat released by the exhaust flue gas to atmosphere. The released heat consists of sensible and latent one. Recently, for a biological and environmental safety, a clean fuel such as a natural gas is widely used in the boiler. As the clean fuel includes a lot of hydrogen instead of carbon, the exhaust flue gas includes a lot of steam accompanying with the latent heat. To reduce the toxic products of combustion, it is preferable to use oxygen instead of air. As a next generation boiler, the oxygen combustion boiler was planned and developed in Japan. The oxygen-combustion flue gas has the larger amount of steam concentration than that in the air-combustion flue gas including nitrogen. So the latent heat recovery from the flue gas is very important to improve the boiler efficiency.

Shown in Fig.1 is the relation between the boiler efficiency and the exhaust gas temperature in the oxygen and air combustion system. The efficiency is larger than 100% at the lower exhaust temperature as the boiler efficiency is defined with a lower heating value of A-heavy oil fuel. The efficiency in the oxygen combustion is much higher than that in the air combustion due to the lack of heat loss carried out with the nitrogen. The dew point of the oxygen-combustion flue gas including the larger amount of steam instead of nitrogen is higher than that in the air-combustion flue gas. The steep increase of efficiency can be observed at the lower temperature region below the dew points. In this lower temperature region, the latent heat in the flue gas is recovered and the efficiency is increased. So the latent heat recovery from the flue gas is very important to improve the boiler efficiency in the oxygen combustion system.

In the previous basic studies¹⁻⁴, condensation heat transfer on horizontal stainless steel tubes has been investigated experimentally by using an actual flue gas from a natural gas boiler. The experiments were conducted using single and 2 stages of tubes at different air ratios and steam mass concentrations of the flue gas in a wide range of tube wall temperature. The condensation heat transfer was well predicted with the simple analogy correlation in the high wall temperature region. In the low wall temperature region less than 30°C or the high steam mass concentration presuming the oxygen combustion, the total heat transfer was higher than that predicted by the simple analogy correlation.

The thermal hydraulic behavior was experimentally studied in a heat exchanger for the

latent heat recovery from a flue gas generated with the combustion of oxygen and A-oil. The steam mass concentration of the flue gas was approximately 25% which value was higher than that of an air-combustion flue gas. The parametric study varying the flue gas and feed water flow rate was conducted. Based on the previous basic studies, a prediction method for the heat exchanger was proposed⁵. In the prediction, the flue gas was treated as a mixture of CO₂, CO, O₂, SO₂ and H₂O, and the one-dimensional heat and mass balance calculation along the flow direction of flue gas was conducted. The heat and mass transfer on tubes was evaluated with a modified analogy correlation proposed in the previous basic study⁴. The modification was proposed to take account of the mass absorption effect at wall in the high steam mass concentration.

The following points are considered to be important in the verification of the calculation method comparing with the present experimental result.

1. Availability of the proposed analogy correlation between heat and mass transfer.
2. Proper estimation for physical properties and diffusivity of actual flue gas.
3. Precise calculation for the white fuming when the gas temperature merges with the saturation temperature.
4. Effect of condensate on heat transfer and pressure loss.
5. Stage by stage calculation method instead of conventional method using a logarithmic difference.

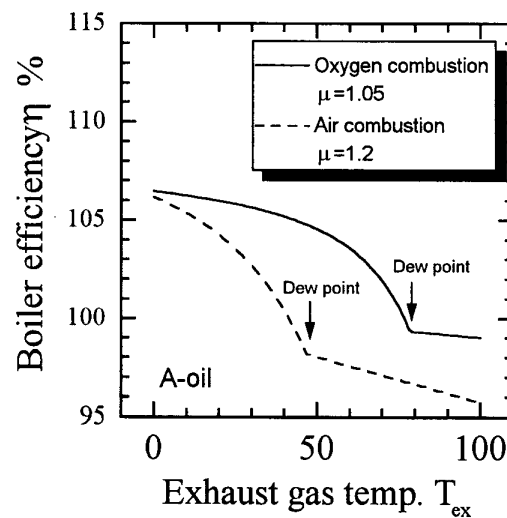


Fig. 1 Boiler efficiency in oxygen and air combustion

EXPERIMENTAL APPARATUS AND METHOD

Shown in Fig.2 is a schematic of experimental apparatus. The heat exchanger consists of 3 staggered banks of 3 rows and 22 stages of bare tubes. The flue gas from an oxygen combustion boiler is led to the upper plenum and flows downward in the first heat exchanger, upward in the second one and downward in the third one. The flue gas was released to atmosphere from the outlet plenum. The 3 tubes at each stage are connected with a header to maintain the same flow rate of feed water. The feed water is supplied at the downstream of gas flow and flows counter-currently to the upstream. The temperature distributions of water and flue gas in the heat exchanger were measured with sheath thermocouples. The thermocouple signals were transferred to a personal computer with a GPIB line and analyzed. The measurement error of the temperature in this study was within ± 0.1 K. The pressure loss and the total amount of condensate generated in the heat exchanger were also measured.

Shown in Fig.3 is the arrangement of heat transfer tubes. The heat exchanger consists of a staggered bank of 3 row tubes and 66 stages in total. The inner and outer diameter of the tube were 21.4 and 25.4mm, respectively. The parametric study varying the flue gas flow rate, feed water temperature and flow rate was conducted. The experimental conditions are shown in Tables.1. The oxygen rate was maintained at approximately 1.07 and the flue gas flow rate was varied with changing the fuel flow rate in the boiler.

CONSTITUTIVE EQUATIONS FOR PREDICTION

Fuel combustion

The properties of A-heavy oil fuel used in the test boiler are shown in Table.2. Volumetric concentrations of CO_2 , SO_2 , O_2 and CO in the dry gas were measured by a gas analyzer. By using the mass flow rate of the fuel V_F , the volumetric flow rate of the carbon dioxide and monoxide, V_{COX} , is

$$V_{\text{COX}} = V_F \cdot \frac{F_C}{F_H} \cdot 22.4 \quad (1)$$

The volumetric flow rate of dry gas V_d is,

$$V_d = \frac{V_{\text{COX}}}{\text{CO}_2 + \text{CO}} \quad (2)$$

The molar fraction of the hydrogen corresponding to CO_x of 1 mol can be calculated as,

$$\text{CHR} = 12 \frac{F_H}{F_C} \quad \text{mol}$$

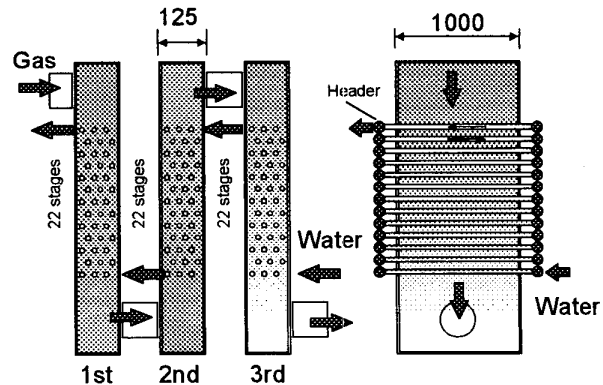


Fig. 2 Schematic of experimental apparatus

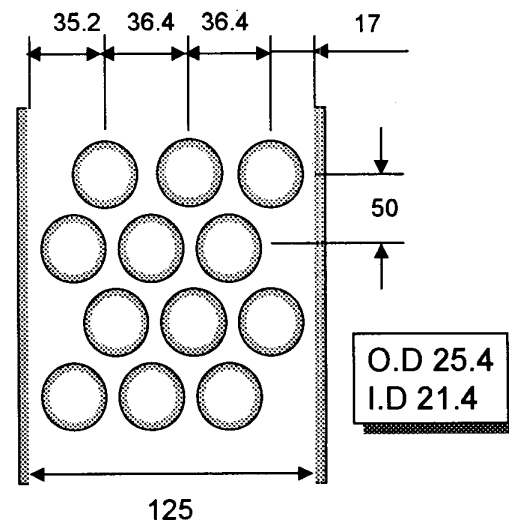


Fig. 3 Arrangement of heat transfer tubes

Table1 Test conditions of bare tube

Test no.	1	2	3	4	5
Oxygen ratio μ	1.07	1.07	1.07	1.07	1.05
Fuel flow rate (kg/h)	178	177	176	120	60.1
Gas inlet temp. ($^{\circ}\text{C}$)	88.2	92.6	95.4	83.3	77.1
Feed water (kg/h)	3000	2500	3700	2000	1000
Water inlet temp. ($^{\circ}\text{C}$)	19.8	19.7	24.6	18.5	21.7

Table 2 Properties of A-heavy oil fuel

	Fraction(kg/kg)
Carbon	$F_C=0.861$
Hydrogen	$F_H=0.131$
Sulfur	$F_S=0.0063$

By using the measured concentration of CO_2 , SO_2 , O_2 and CO , the air ratio μ is calculated as

$$\mu = 1 + \frac{O_2 - 0.5CO}{(1 + CHR/4)(CO_2 + CO) + SO_2} \quad (3)$$

The volumetric fraction of H_2O in the flue gas can be estimated as

$$H_2O = \frac{(CO_2 + CO) \cdot CHR / 2}{1 + (CO_2 + CO) \cdot CHR / 2} \quad (4)$$

The volumetric flow rate of wet gas, V_{wt} , is

$$V_{wt} = \frac{V_d}{1 - H_2O} \quad (5)$$

When the flue gas temperature is T_f °C, the steam mass concentration C_f per unit volume of flue gas is,

$$C_f = \frac{H_2O \cdot 18}{22.4} \cdot \frac{273.15}{273.15 + T_f} \quad (6)$$

The steam mass concentration W_f per unit mass of flue gas is

$$w_f = \frac{H_2O \cdot 18}{H_2O \cdot 18 + (1 - H_2O)(CO_2 \cdot 44 + CO \cdot 28 + SO_2 \cdot 64 + O_2 \cdot 32)} \quad (7)$$

Heat and mass transfer in gas side

The total heat flux q_T consists of the convection heat flux q_V and the condensation heat flux q_C as

$$q_T = q_V + q_C \quad (8)$$

The convection heat flux is expressed as

$$q_V = h_V(T_f - T_w) \quad (9)$$

The condensation heat flux q_C can be expressed as,

$$q_C = h_C L_W (C_f - C_w) \quad (10)$$

where C_w is the mass concentration of saturated steam at the wall temperature T_w . Based on the previous studies, the Nusselt number Nu_f for the average convective heat transfer coefficient in the range of $10^3 < Re_f \leq 2 \times 10^5$ is

$$Nu_f = c Re_f^{0.6} Pr_f^m (Pr_f / Pr_w)^{0.25} \quad (11)$$

Zukauskas⁶ proposed $m=0.36$ and

$$\text{For } S_1/S_2 < 2 \quad c = 0.35(S_1/S_2)^{0.2} \quad (12)$$

$$\text{For } S_1/S_2 \geq 2 \quad c = 0.40 \quad (13)$$

for a staggered bank. For the condensation of steam on heat transfer tubes, the modified Sherwood number taking account of the mass absorption effect on the wall was proposed⁴.

$$Sh_f = \frac{1}{1 - w_i} \left(\frac{1 - w_i}{1 - w_f} \right)^m c Re_f^{0.6} Sc_f^m (Sc_f / Sc_w)^{0.25} \quad (14)$$

Flue gas was treated as a mixture of CO_2 , SO_2 , O_2 , CO and H_2O and its property was estimated with special combinations of each gas property proposed by the previous studies⁷. For example, the heat conductivity and the viscosity were estimated with the methods by Lindsay & Bromley⁸ and Wilke⁹, respectively. It is considered that a strong correlation exists between the thermal and mass diffusivities. As a first attempt, the mass diffusivity of steam in flue gas was estimated with the well-known mass diffusivity of steam in air as

$$D = D_{air} \left(\frac{\kappa}{\kappa_{air}} \right) \quad (15)$$

where κ and κ_{air} are the thermal diffusivities of flue gas and air, respectively. The diffusivity of steam in air can be expressed as¹⁰,

$$D_{air} = 7.65 \times 10^{-5} \frac{(T + 273.15)^{11/6}}{P} \quad (16)$$

The one-dimensional heat and mass balance calculation along the flow direction of flue gas was conducted. The steam mass concentration and the flue gas temperature at $N+1$ th stage can be calculated from those at N th stage as shown in Fig. 4.

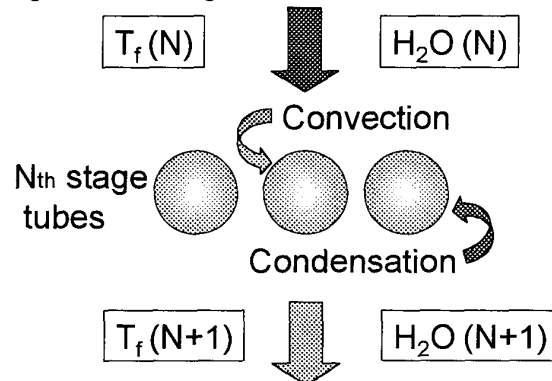


Fig. 4 One-dimensional calculation

The heat and mass balance equations are;

$$H_2O(N+1) = \frac{H_2O(N) \cdot V - \frac{q_C A_W}{L_W} \cdot \frac{22.4}{18}}{V - \frac{q_C A_W}{L_W} \cdot \frac{22.4}{18}} \quad (17)$$

$$T_f(N+1) = T_f(N) - \frac{q_V A_W}{C_{Pf} \rho_f (273.15 + T_f) / 273.15 \cdot V} \quad (18)$$

where A_w is the heat transfer area per a stage.

It is possible that the gas temperature merges with the dew point which is the saturation temperature corresponding to the partial pressure of steam in the flue gas. When the gas temperature decreases below the dew point, the condensation of steam in the flue gas takes place and the latent heat increases the gas temperature until the gas temperature coincides with the dew point. In this case, the energy balance gives the relation between the increase of the gas temperature, ΔT_f , and the decrease of steam concentration, ΔH_2O , as;

$$\Delta T_f = \frac{18}{22.4} \cdot \frac{L_W}{C_{Pf} \rho_f (273.15 + T_f) / 273.15} \cdot \Delta H_2O \quad (19)$$

Heat conduction in tube

The heat conductivity for the inconel or austenite stainless steel is given with the following approximate correlation¹¹.

$$\lambda_t = 13.2 + 0.013 T_t \quad W/(m K) \quad (20)$$

where T_t is the average temperature of tube as,

$$T_t = \frac{T_w + T_{wi}}{2} \quad (21)$$

where T_w and T_{wi} are the outer and inner wall temperatures, respectively. The heat flux at the outer wall is,

$$q_w = \frac{2\lambda_t(T_w - T_{wi})}{d_o \ln(d_o / d_i)} \quad (22)$$

Heat transfer in water side

Heat transfer correlation by Dittus-Boelter taking account of the pipe inlet region is used. The coefficient by McAdams¹² is used for the modification.

$$Nu = 0.023 Re^{0.8} Pr^{0.4} \left(1 + \left(\frac{d_i}{L} \right)^{0.7} \right) \quad (23)$$

where L is the heating length of tube.

Pressure loss calculation

The pressure loss per a stage of tube is,

$$\Delta P = 2f \rho_f u^2 \quad (24)$$

For the staggered bank of bare tube, Jacob¹³ proposed the following coefficient f ,

$$f = \left[0.25 + \frac{0.118}{\left\{ \left(\frac{S_1}{d_o} \right) - 1 \right\}^{1.08}} \right] Re_f^{-0.16} \quad (25)$$

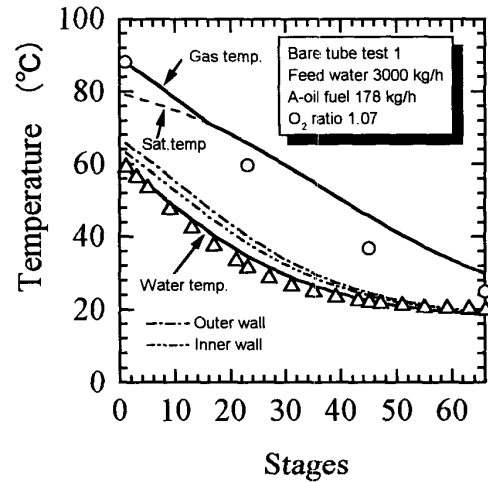


Fig. 5 Test 1 at feed water flow rate of 3000kg/h and fuel flow rate of 178 kg/h

COMPARISON OF EXPERIMENTAL RESULT AND PREDICTION

Temperature distribution

Shown in Fig.5 is the comparison of the experimental result and the prediction at the feed water of 3000 kg/h and flue gas flow rate of 178 kg/h. The solid lines are the temperatures of gas and water in the bank. The a-dot-dashed line and the two-dots-dashed line are the inner and outer wall temperature of tubes, respectively. The dashed line is the saturation temperature (dew point) corresponding to the partial pressure of steam in the flue gas. As the outer wall temperature is smaller than the dew point, the condensation on the wall takes place throughout the heat exchanger. The dew point decreases with increasing stages as the steam concentration decreases. The key O and Δ are the measured temperatures of gas

and water, respectively. The prediction for the water temperature agrees well with the experimental result. The prediction for the gas temperature is slightly higher than the experimental result. In these experiments of the high fuel flow rate, the dispersed condensate in the flue gas tends to wet the thermocouples to measure the gas. The wet thermocouples indicate the lower value than the gas temperature.

Shown in Fig.6 is the calculation result for the same experiment as Fig.5 considering the heat resistance of condensate on the tubes. The calculated gas and water temperature slightly rise due to the heat resistance of condensate. Figure7 is the calculated average thickness on the tubes. The average thickness was obtained by the calculation method shown in APPENDIX. It is assumed that all the generated condensate flows on the tubes in the calculation. The maximum thickness is approximately 0.17mm. The temperature difference between the film is less than 2.5K. The existence of the film did not affect the calculated temperature profiles in the bank.

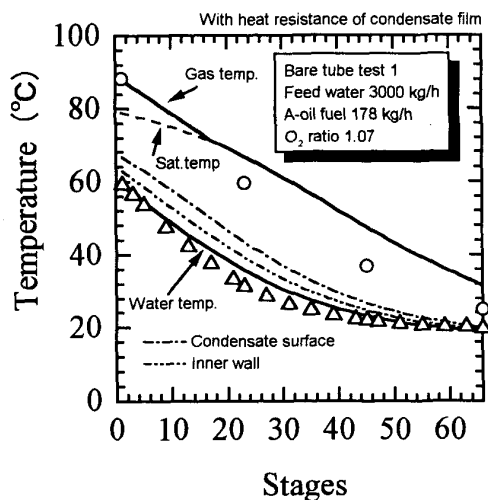


Fig. 6 Effect of heat resistance of condensate

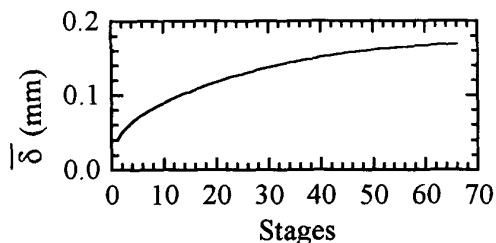


Fig. 7 Calculated average film thickness

The effect of condensate film on the tubes was considered to be negligibly small for the heat and mass transfer calculation.

Shown in Figs.8 and 9 are comparison of the experimental result and prediction when the fuel and feed water flow rate were reduced. In Test 4 in Fig.8 and Test 5 in Fig.9, the fuel flow rates were reduced to 67 and 34% of the full load test 1, respectively.

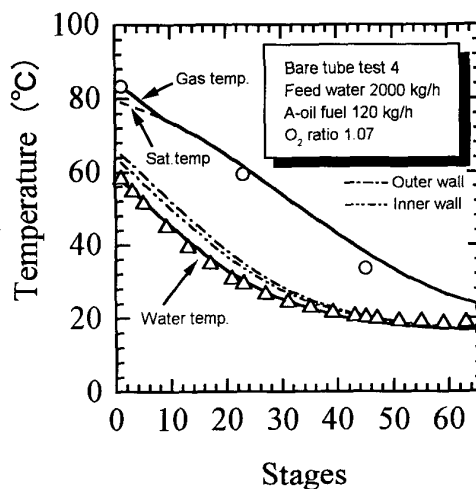


Fig. 8 Test 4 at feed water flow rate of 2000kg/h and fuel flow rate of 120 kg/h

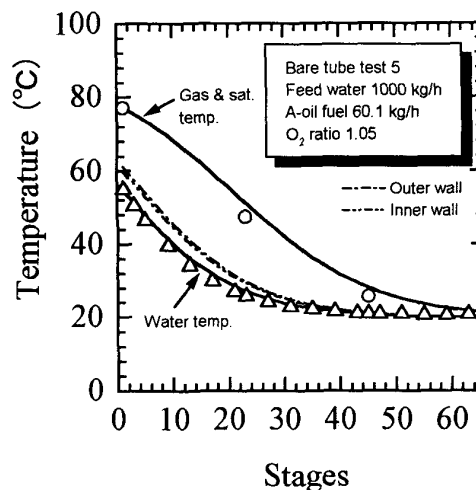


Fig. 9 Test 5 at feed water flow rate of 1000kg/h and fuel flow rate of 60.1 kg/h

As the flue gas flow rate and the amount of condensate is comparatively small in these tests, the effect of the wet thermocouple is considered to be negligible. The measured gas temperature agrees well with the prediction. This result also indicates the precise calculation for the white fuming condition when the saturation and gas temperature merge.

Shown in Fig.10 is the calculated condensation rate m_{CS} at each stage in the full load test 1 and the reduced load tests 4 and 5. The condensation rate takes a peak at the inlet of heat exchanger and decreases gradually with increasing stage.

Pressure loss and amount of condensate

Shown in Fig. 11 is the comparison of experimental result and prediction for the pressure loss throughout the heat exchanger. Though the empirical correlation obtained in the non-condensing region was used in the one-dimensional calculation, the experimental results for the banks of bare and finned tubes agreed well with the prediction. The effect of condensate film on the tubes was considered to be negligibly small for the pressure loss calculation.

Shown in Fig.12 is the predicted and measure amount of condensate at each heat exchange. The prediction slightly underestimates the generated amount at the first exchanger and slightly overestimates those at the second and third exchanger.

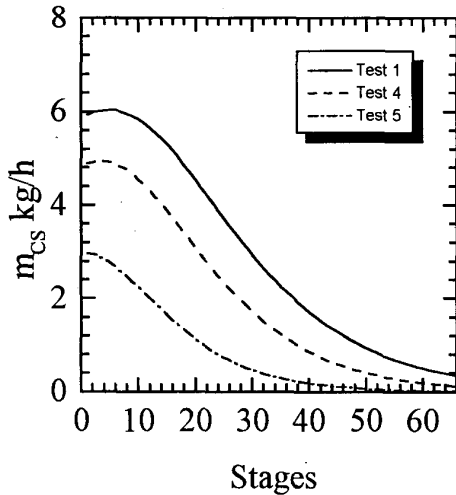


Fig. 10 Condensation flow rate at each stage

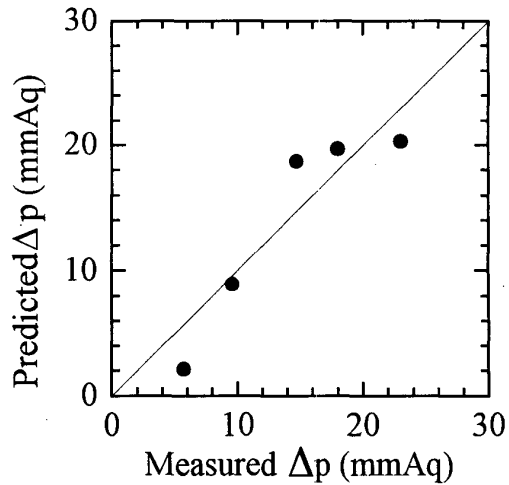


Fig. 11 Pressure difference between inlet and outlet of heat exchanger

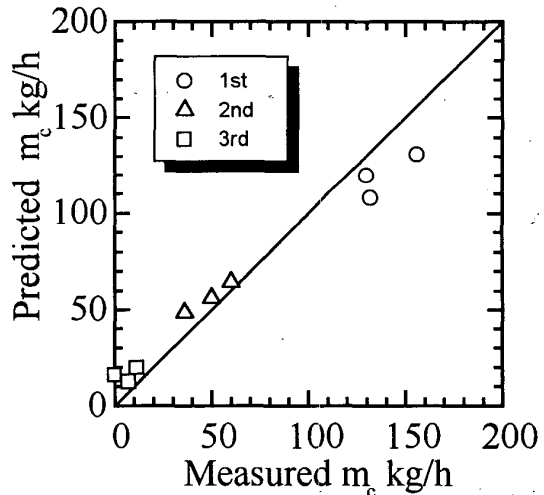


Fig. 12 Predicted and measured amount of condensate at each exchanger

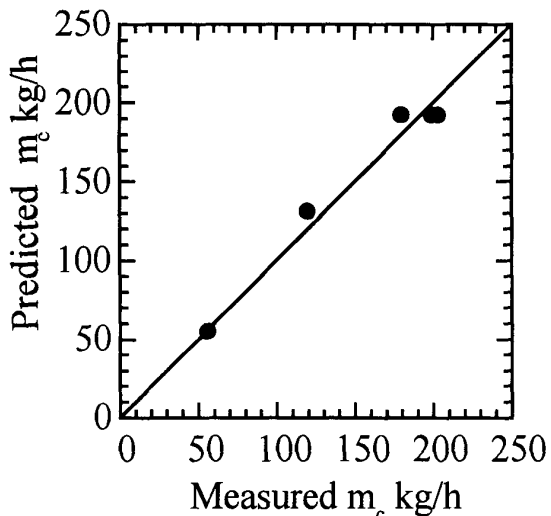


Fig. 13 Predicted and measured total amount of condensate

Shown in Fig. 13 is the comparison of experimental result and prediction for the amount of condensate throughout the heat exchanger. The total amount of condensate generally agrees well with the one-dimensional mass and heat balance calculation.

CONCLUSION

Thermal-hydraulic behavior of heat exchangers for the latent heat recovery was investigated experimentally by using an actual flue gas from an oxygen combustion boiler. The parametric study varying the flue gas flow rate, feed water temperature and flow rate was conducted. Based on the previous basic studies, a prediction method for the heat exchanger was proposed. In the prediction, the flue gas was treated as a mixture of CO_2 , CO , O_2 , SO_2 and H_2O , and the one-dimensional heat and mass balance calculation along the flow direction of flue gas was conducted. The heat and mass transfer on tubes was evaluated with the modified analogy correlation. When the gas temperature decreased below the dew point, the condensation of steam in the flue gas took place and the released latent heat increased the gas temperature until the gas temperature coincided with the dew point. The effect of condensate film on the tubes was considered to be negligibly small for the heat transfer and pressure loss calculation. The experimental results for the temperature distributions of water and flue gas in the test heat exchangers with bare tubes agreed well with

the prediction.

ACKNOWLEDGMENT

The author appreciates the helpful supports by Takao Iron Works Co. Ltd., The Japan Society of Industrial Machinery Manufacturers and NEDO (New Energy and Industrial Technology Development Organization of Japan).

REFERENCES

1. Osakabe, M., Ishida, K., Yagi, K., Itoh, T. and Ohmasa, M., 1998, "Condensation heat transfer on tubes in actual flue gas (Experiment using flue gas at different air ratios)", (in Japanese), *Trans. of JSME*, 64-626, B, 3378-3383
2. Osakabe, M., Yagi, K., Itoh, T. and Ohmasa, M., 1999, "Condensation heat transfer on tubes in actual flue gas (Parametric study for condensation behavior)", (in Japanese), *Trans. of JSME*, 64-626, B, 3378-3383
3. Osakabe, M., K., Itoh and T. Ohmasa, 2000, "Condensation heat transfer on spirally finned tubes in actual flue gas", (in Japanese), *J. of MESJ*, 35-4, 260-267
4. Osakabe, M., Itoh, T. and Yagi, K., 1999, "Condensation heat transfer of actual flue gas on horizontal tubes", *Proc. of 5th ASME/JSME Joint Thermal Eng. Conf., AJTE99-6397*
5. Osakabe, M., 1999, "Thermal-hydraulic behavior and prediction of heat exchanger for latent heat recovery of exhaust flue gas", *Proc. of ASME, HTD-Vol.364-2*, 43-50
6. Zukauskas, A., 1972, *Advances in Heat Transfer*, 8, Academic press, New York, 93-160
7. JSME, 1983, *Data Book: Heat Transfer 3rd Edition*, (in Japanese)
8. Lindsay, A.L. and Bromley L.A., 1950, "Thermal conductivity of gas mixtures", *Indust. Engng. Chem.*, 42, 1508-1510
9. Wilke, C.R., 1950, "A viscosity equation for gas mixture", *J. Chem. Phys.*, 18, 517-519
10. Fujii, T., Kato, Y and Mihara, K., 1977, "Expressions of transport and thermodynamic properties of air, steam and water", *Univ. Kyushu Research Institute of Industrial Science Rep.66*, 81-95
11. Osakabe, M., 1989, "Thermal-hydraulic study of integrated steam generator in PWR", *J. Nucl. Sci. & Technol.*, 26(2), 286-294
12. McAdams, W.H., 1954, *Heat transmission*,

McGRAW-HILL

13. Jakob, M., 1938, "Heat transfer and flow resistance in cross flow of gases over tube banks", *Trans. ASME*, 60, 384

APPENDIX

Though a part of condensate falls down between the tubes and on the duct wall, it is assumed that all the condensate generated at the upper stage flows on the tubes as a laminar film. The momentum balance dominated by viscous and gravity force gives the velocity distribution at θ° from the tube top:

$$u = \frac{(\rho_L - \rho_G)g \sin \theta}{\mu_L} \left(y\delta - \frac{y^2}{2} \right) \quad (26)$$

Integrating the above velocity profile and using the condensate mass flow rate per unit of tube length, m , yields

$$\delta = \left[\frac{1.5\mu_L m}{\rho_L(\rho_L - \rho_G)g \sin \theta} \right]^{1/3} \quad (27)$$

The heat conductivity of film is

$$K = \frac{\lambda_L}{\delta} = \left[\frac{\lambda_L^3 \rho_L(\rho_L - \rho_G)g \sin \theta}{1.5\mu_L m} \right]^{1/3} \quad (28)$$

The average conductivity from $\theta=0^\circ$ to $\theta=\pi$ is

$$\bar{K} = \frac{1}{\pi} \int_0^\pi K d\theta = 0.72 \left[\frac{\lambda_L^3 \rho_L(\rho_L - \rho_G)g}{\mu_L m} \right]^{1/3} \quad (29)$$

The average heat resistance of film is defined as the inverse of the above average conductivity. The average film thickness is

$$\bar{\delta} = \frac{\lambda_L}{\bar{K}} \quad (30)$$

In the calculation, the mass flow rate, m , at a certain stage includes the condensate generated at the stage for the conservative estimation.

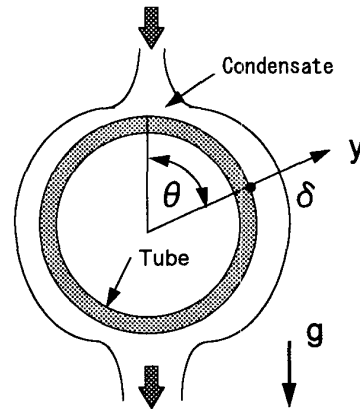


Fig. 14 Heat conductance of condensate film